Deep–Sea Research I 172 (2021) 103487

Contents lists available at ScienceDirect

Deep-Sea Research Part I

journal homepage: http://www.elsevier.com/locate/dsri

Rock magnetic variability of quaternary deep-sea sediments from the Bering Sea and their environmental implications

Steve Lund [a,*], Emily Mortazavi [a], Ellen Platzman [a], Matt Kirby [b], Joe Stoner [c], Makoto Okada [d]

[a] Department of Earth Sciences, University of Southern California, University Park, Los Angeles, CA 90089-0740, USA
[b] Department of Geology, California State Univ., Fullerton, CA, USA
[c] College of Ocean and Atmospheric Sciences, Oregon State University, Corvallis, OR, USA
[d] Department of Earth Sciences, Ibaraki University, Ibaraki, Japan

ARTICLE INFO

Keywords:
Bering sea
Rock magnetism
Deep sea sedimentation
Quaternary climate

ABSTRACT

IODP Ex. 323 shipboard rock magnetic measurements of Quaternary deep-sea sediments from the Bering Sea identified a dramatic bimodal character to the sediments, alternating between sediments with strong natural magnetic remanence (NRM) and magnetic susceptibility (chi) and those with order-of-magnitude lower values. We now generally associate the high-magnetic-intensity sediments with interglacial/interstadial times and the low-magnetic-intensity intervals are generally associated with glacial/stadial conditions. This pattern can be largely correlated among all seven IODP Ex. 323 sites. We have now completed more detailed rock magnetic measurements on selected u-channeled sediments from these sites. U-channel rock magnetic measurements indicate that the high-intensity sediments contain relatively coarser magnetic grains (sand/silt) associated with coarser siliciclastic sediments while the low-intensity sediments contain finer magnetic grains (silt) associated with finer siliciclastic sediments. We associate the coarser magnetic grains and overall coarser clastic sediments with warmer intervals when more open water conditions permit sediment flux from the continental shelves. The finer magnetic grains and associated finer clastic sediment are largely derived from sediment reworking and redeposition associated with slope processes and deep-sea contour currents when ice cover was more permanent. We have corroborated the grain size variability with magnetic hysteresis measurements and clastic grain size analysis. The clastic grain size distributions of the coarser versus finer grained sediments are significantly different; coarser grained sediments have a broad grain size distribution with 50–60 μm mean grain size, while finer grained sediments have a much more narrow grain size distribution with 15–20 μm mean grain size. The finer grain size distribution is consistent in range and mean grain size to North Atlantic deep-sea sediment deposited as drift deposits by contourite deposition (Heezen and Ruddiman, 1966; Johnson et al., 1988). The dominant magnetic mineral in all sediments is detrital magnetite. Early sediment diagenesis plays a minor role in the overall rock magnetic variability of the Bering Sea deep-sea sediments due to the overall large clastic grain size. The magnetic variability that we see in the Quaternary Bering Sea sediments appears to be comparable to other studies from this region. VanLaningham et al. (2009) attribute deposition of the Meiji drift, directly south of the deep-water exit from the Bering Sea, to sediments derived from the Bering Sea. They see a bimodal distribution in the types of sediments that are deposited with younger arc rocks during interglacials and older continental rocks during glacials. That is consistent with our coarser Interglacial magnetic sediments derived primarily from shelf rocks rich in recent volcanics versus deeper Bering Sea sediments associated with reworking of older Bering Sea sediments during the glacials. We also note the strong similarity in timing of strong versus weak magnetic intensity sediments of Lake Elgygytgyn, about 1000 km to the NW of the Bering Sea, Both seem to be controlled by the degree of intermittent open water conditions, more so in the interglacials and very little in the glacials, but operating on a finer scale than simple glacial/interglacial cycling.

* Corresponding author.
E-mail address: slund@usc.edu (S. Lund).

https://doi.org/10.1016/j.dsr.2021.103487
Received 15 December 2020; Accepted 31 January 2021
Available online 11 March 2021

1. Introduction

Integrated Ocean Drilling Program (IODP) Expedition 323 (Takahashi et al., 2011) cored Quaternary and Pliocene deep-sea sediments at seven sites in the Bering Sea (Fig. 1). Four of the sites (U1339, U1343, U1344, U1345) are located along the northern Bering Sea margin and are termed Bering Slope sites (1008–3184 m water depth); three of the sites (U1340, U1341, U1342) are located in the south central Bering Sea along the deep-sea Bowers Ridge and are termed the Bowers Ridge sites (837–1870 m water depth). All seven sites share a depositional history that relates to continental runoff from Alaska, ocean circulation in the Bering Sea (e.g., Takahashi, 2005) and its connections to more large-scale Northern Pacific circulation, which are all driven by climate changes (Tanaka and Takahashi, 2005).

The sediments are predominantly either siliciclastic sediments or biogenic sediments (Takahashi et al., 2011; Aiello and Ravelo, 2012). The siliciclastic material may come from either the margins of the Bering Sea, mostly to the North, or from intermediate to deep ocean currents that variably scour and re-deposit deep-sea sediments (Sharma, 1975; Nagashima et al., 2012; Wegner et al., 2015). The siliciclastic material derived from the margins is a mixture of medium-sorted shelf sediment (normal suspended load, distal storm deposits, distal turbidites), minor aeolian sediment, and more poorly sorted ice-rafted debris (IRD) (Sharma, 1975; Seibold and Berger, 1996; Sommerfield et al., 2007). The magnetic mineralogy is presumably a mixture of continental-derived detrital grains (containing both ferric and ferrous iron minerals, mostly magnetite) and some authigenic ferric minerals (goethite, hematite) derived from oxic weathering on the continent or shelf. Any re-worked deep-sea siliciclastic sediments (excepting IRD contributions) should be more well-sorted with a mean grain size depending on bottom current speed or proximity to the slope (Joseph et al., 1998), but typically finer-grained than shelf-derived siliciclastic material (e.g., Carlson and Karl, 1985; Seibold and Berger, 1996).

2. Shipboard rock magnetic measurements

Shipboard magnetic measurements were made on all cores collected using a pass-through long-core 2G cryogenic magnetometer. The normal sequence was to measure the initial natural remanence (NRM) in at least one hole at each site. The NRMs were then step-wise demagnetized in alternating magnetic fields at 10 mT and 20 mT to assess the relative strength and ease of removal of a viscous remanence (VRM), which is ubiquitously present in IODP cores (e.g., Lund et al., 2003). Shipboard measurements at 20 mT appeared to effectively remove the VRM. Other holes were commonly only demagnetized at 20 mT. Long-core magnetic susceptibility was measured on all cores and used as a shipboard correlation tool for developing a composite stratigraphic sequence at each site. The shipboard rock magnetic results are presented in Takahashi et al. (2011).

The rock magnetic intensities of Quaternary sediments from the Bering Sea vary significantly on order-of-magnitude intensity scales. Fig. 2 shows shipboard measurements of magnetic susceptibility (chi) and natural remanence (NRM) intensities for Sites U1340 and U1344 during the Brunhes Epoch (0–780,000 YBP). The magnetic susceptibility (chi) and natural remanence (NRM) intensities are strong, on average, but undergo dramatic order-of-magnitude steps, with quite sharp breaks, between high and low values at a ~5–20 m wavelength. The original shipboard hypothesis was that high magnetic intensities were associated with coarser glacial sediment due to enhanced flushing of shelf sediment into the deep basin associated with low sea levels. Low magnetic intensities were associated with finer interglacial sediment due to trapping of coastal sediments in the shelf associated with high sea levels.

Rock magnetic variations reflect changes in magnetic mineralogy, concentration, and grain size in sediments. If most rock magnetic variability is due to changes in sediment type/lithology, then the rock magnetic variations are a good proxy for variations in the overall siliciclastic sediment lithology (e.g., Lund et al., 1992). If some part of the rock magnetic variations is due to chemical changes in the sediment, then these conclusions are more uncertain (Roberts, 2015). This pattern of oscillating high/low magnetic intensity is consistent with the glacial-interglacial pattern generally observed in the North Atlantic Ocean (Heezen et al., 1966; Johnson et al., 1988; Keigwin and Jones, 1989; Keigwin and Jones, 1989) associated with finer grained lower magnetic intensity interglacial sediments versus coarser grained higher magnetic intensity glacial sediments. More recent oxygen isotope stratigraphy of the IODP Ex. 323 sediments (Asahi et al., 2016; Cook et al., 2016) indicates, however, that the opposite pattern of timing is more likely in the Bering Sea. High (low) magnetic intensities are normally associated with interglacial (glacial) intervals. However, the oscillation

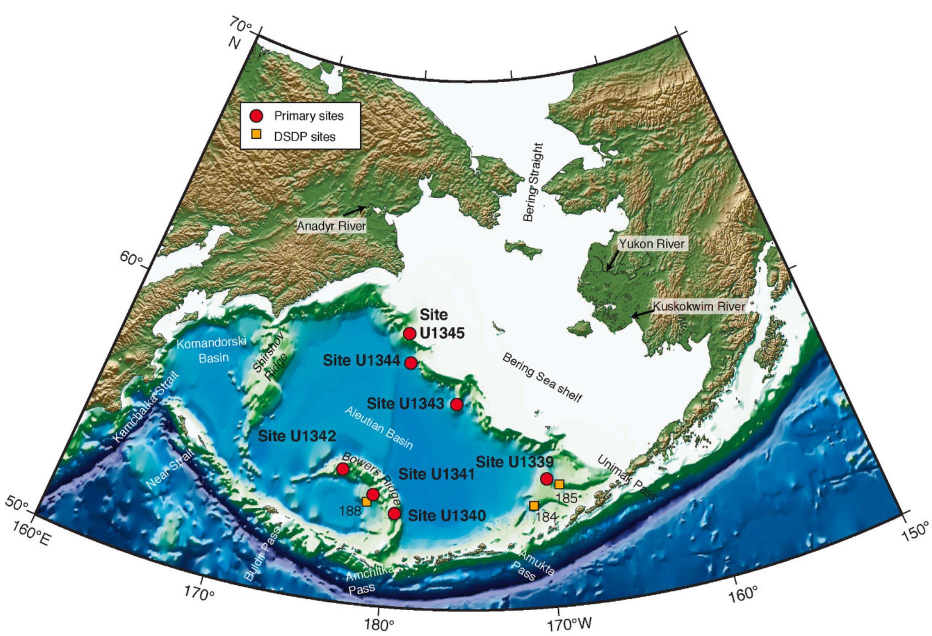

Fig. 1. Map of the Bering Sea showing the location of IODP Expedition sites U1339–U1345.

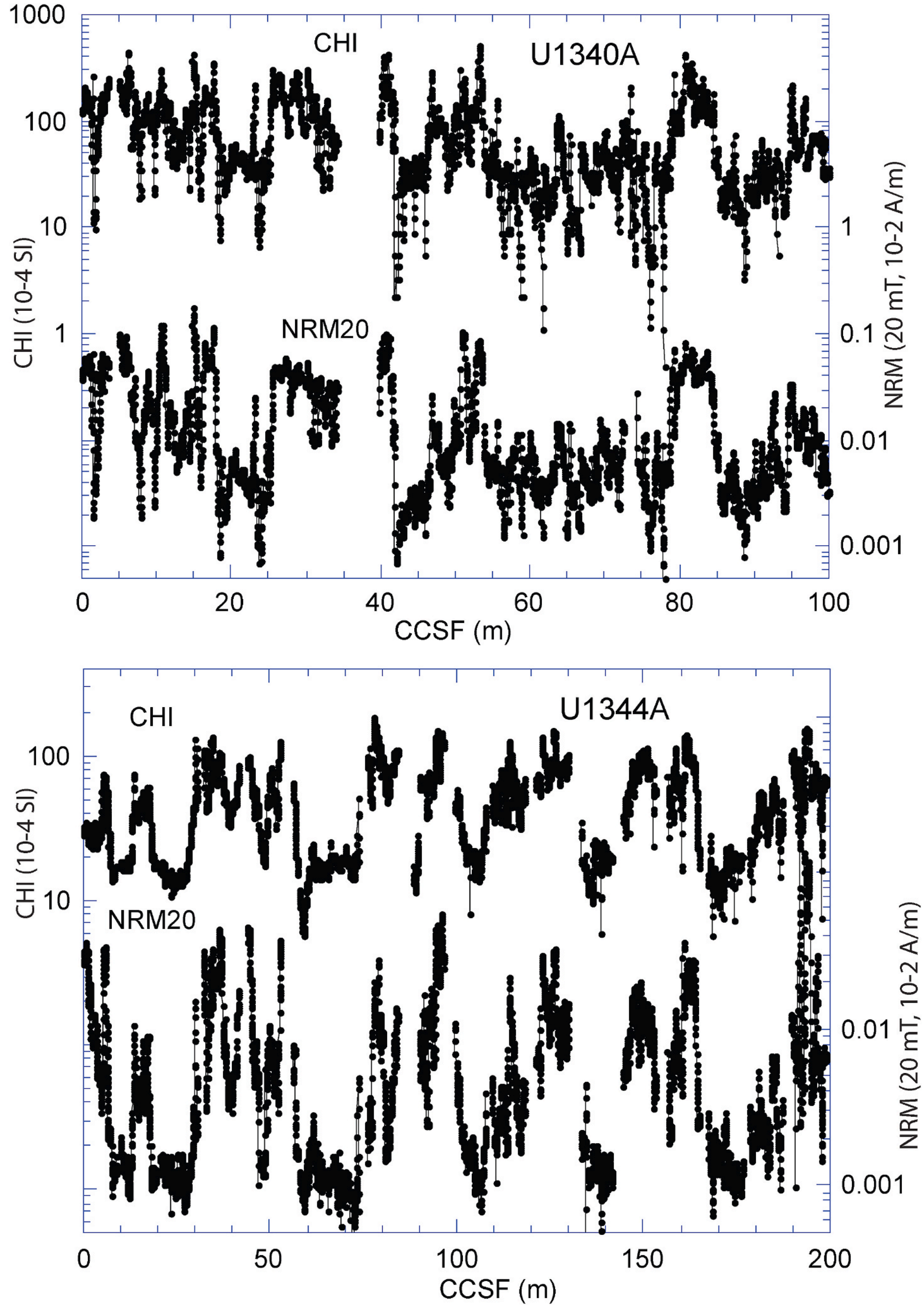

Fig. 2. Rock Magnetic stratigraphy for the Brunhes Epoch intervals of Sites U1340 (top) and U1344 (bottom). Magnetic susceptibility (chi) is shown at top in each figure and natural remanence (NRM) after 20 mT af demagnetization is shown at bottom.

pattern occurs too frequently to be a simple glacial/interglacial stage oscillation and must indicate that sub-stage variability in sedimentation is prevalent as well.

3. U-channel rock magnetic measurements

We have now carried out new magnetic measurements on selected cores from IODP Expedition 323 using u-channels. U-channels remove a column of sediment, 2 × 2 cm in cross section, from the split face of a core. These u-channels should provide the most undisturbed sediment for magnetic measurements. U-channels are taken from the same cores that were used for the shipboard paleomagnetic studies. For this paper, we study u-channel rock magnetic measurements from the uppermost 30 m of Sites U1339, U1340, U1341, U1343, U1344, and U1345 (Fig. 1).

The natural remanence (NRM) of all u-channels were initially measured, using the Oregon State University 2G cryogenic magnetometer, at 20-mT af demagnetization and then step-wise af demagnetized at 10 mT steps up to 100 mT. Initial analysis of the NRM is summarized in Lund et al. (2016). Then selected u-channels were given an artificial anhysteretic remanence (ARM, 0.5 mT steady field, 100 mT af field) and measured. Then the ARMs were stepwise demagnetized at 10, 20, NS 40 mT and remeasured. Finally, an isothermal remanence (IRM, 1 T steady field) was applied to each u-channel and measured. Then the IRMs were stepwise demagnetized at 10, 20, NS 40 mT and remeasured. These detailed rock magnetic measurements can be used to assess the magnetic mineral concentration, composition, grain size, and evidence for early sediment diagenesis/authigenesis in all cores.

Fig. 3 shows a blow-up of the rock magnetic intensity variability at

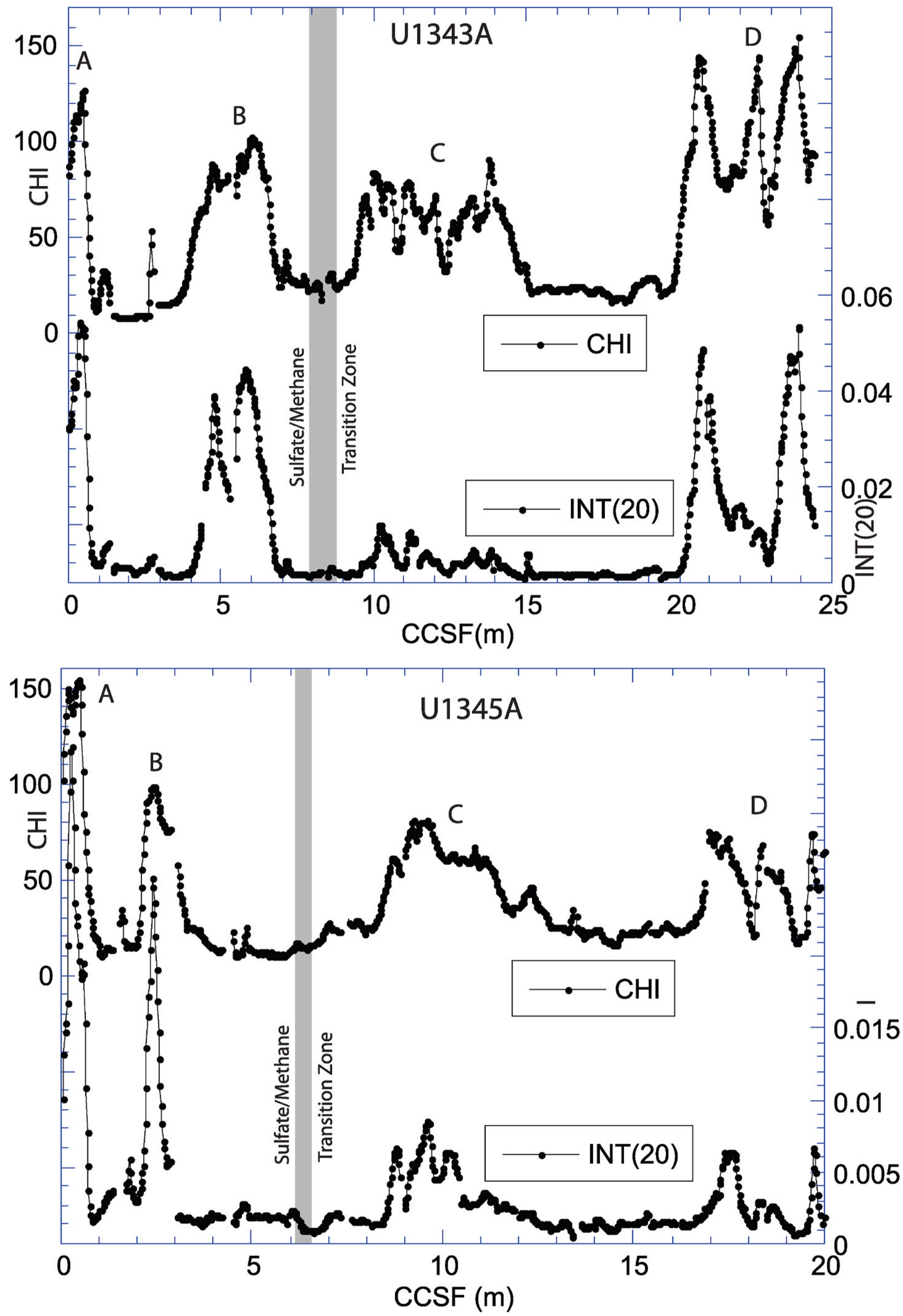

Fig. 3. Expanded rock magnetic stratigraphy (chi, NRM) for the last ~100,000 years at sites U1343 and U1345. High intensity intervals are labeled A-D. A corresponds to Stage 1, B to the Younger Dryas, C to Stage 3, and D to Stage 5 A-C. This pattern is correlatable among all of the Bering Slope sites.

Sites U1343 and U1345 for the last glacial cycle (~last 100,000 years; Asahi et al., 2016; Cook et al., 2016) based on u-channel measurements. The pattern of intensity oscillation noted in Fig. 2 is clearly apparent. Four clear intensity highs are labeled in Fig. 3, which alternate with broad intervals of intensity lows. Feature A is Holocene in age (<9 ka), feature B is associated with the Younger Dryas (~11.5–13 ka), feature C is centered in oxygen-isotope Stage 3 (24–59 ka), and feature D is associated with late Stage 5 (~71–100 ka). The ages are assigned based on oxygen isotope measurements at Site 1345 (Cook et al., 2016). Features A, C, and D are interstadial to interglacial intervals. They are associated with high magnetic intensity, opposite to our shipboard assumption. This pattern of intensity oscillation appears to be correlatable among the Bering Slope sites and probably the Bowers Ridge sites (Lund et al., 2016); it suggests that regional climate/environmental variability is a significant factor in the variation. High magnetic intensities (presumably due to high magnetic and overall clastic concentrations) are generally associated with relatively warm (interglacial/interstadial) conditions and lower magnetic intensities are generally associated with colder (glacial/stadial) conditions. Fig. 3 also shows the location of the sulfate/methane transition zone (SMTZ) in porewater geochemistry (Takahashi et al., 2011; Wehrmann et al., 2011). Below, we will assess the role of early sediment diagenesis/authigenesis in the development of these intensity patterns.

Our u-channel rock magnetic data suggest that the high magnetic intensity sediments are associated with relatively coarse-grained siliciclastic sediments (sands/silts); but these sediments also commonly include significant (often times >50%) biogenic components (Takahashi et al., 2011; Aiello and Ravelo, 2012). Fig. 4 shows two rock magnetic estimates of magnetic grain size in the surface sediments of Site 1345. The ratio of ARM/chi is traditionally used to indicate magnetic grain size variations in a sequence of generally uniform sediments (e.g., King and Channell, 1991). Higher (lower) values of ARM/chi indicate finer-grained (coarser-grained) magnetic material. It is normal to consider this variability to reflect the overall clastic fraction of a sediment sequence.

Demagnetization of the ARM and SIRM provides another estimate of magnetic grain size variations. As ARM and SIRM are demagnetized in increasing af magnetic fields, the faster the ARM or SIRM intensity loss indicates coarser magnetic material. So ratios of ARM or SIRM intensity at two different levels of demagnetization should estimate magnetic grain size. We have plotted ARM40/ARM20 (ARMs demagnetized at 40 or 20 mT) in Fig. 4. Higher (lower) values of ARM40/ARM20 indicate relatively finer (coarser) grained magnetic material. Both rock magnetic grain size indicators suggest that sediment in high magnetic intensity regions B and C have coarser grained sediment and visa versa. In general, we associate higher magnetic intensity sediments with coarser grained magnetic material and interglacial/interstadial conditions. This general, almost bimodal pattern of physical sedimentation, is typical of all, at least, late Quaternary sediments of the Bering Sea.

4. Hysteresis measurements of rock magnetic variability

Magnetic hysteresis measurements were run on small sediment flakes from selected samples of U1345 using a Princeton measurements AGM housed at USC to further assess the rock magnetic character of the Bering Sea sediments. Samples were measured in a peak magnetic field of 0.7 T. All samples required small to insignificant slope correction implying very little paramagnetic contribution to the magnetic assemblage. Key parameters that were measured include induced magnetization at 0.7 T (Ms), remanent magnetization at 0 T after Ms is reached (Mr), coercivity (Hc), and coercivity of remanence (Hcr).

Fig. 5 (top) shows Mrs, Ms, Hcr, and Hc as a function of depth in U1345. The dashed vertical line in Fig. 5 (top) indicates the boundary between high magnetic intensity sediments at the surface (region A) and low magnetic intensity sediments below (Fig. 4). The high (low) magnetic intensity sediments have higher (lower) Mr and Ms, indicative of

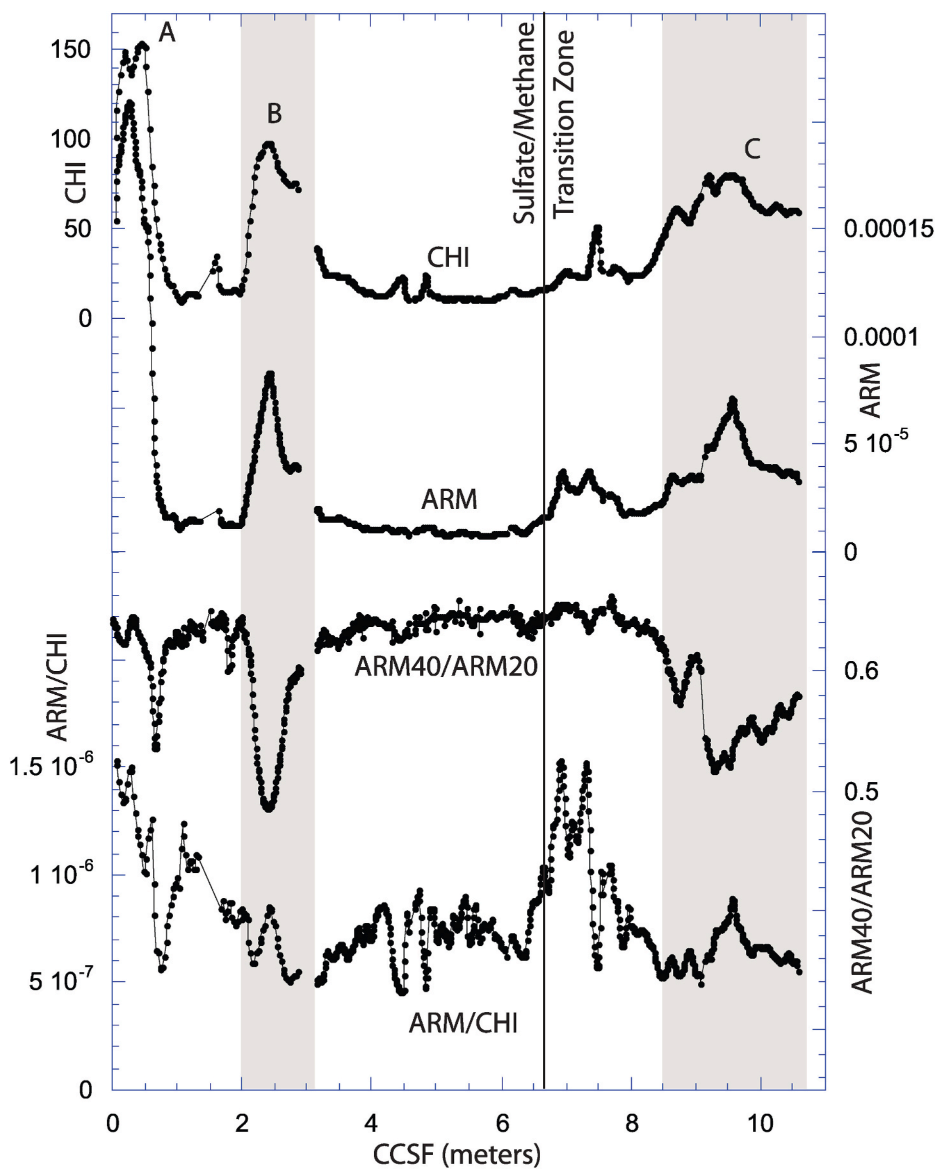

Fig. 4. Detailed rock magnetism of the uppermost 10 m of Hole U1345A. High intensity regions B and C (see Fig. 3) have coarser-grained magnetic minerals present, while the intervening low intensity intervals have finer-grained magnetic minerals.

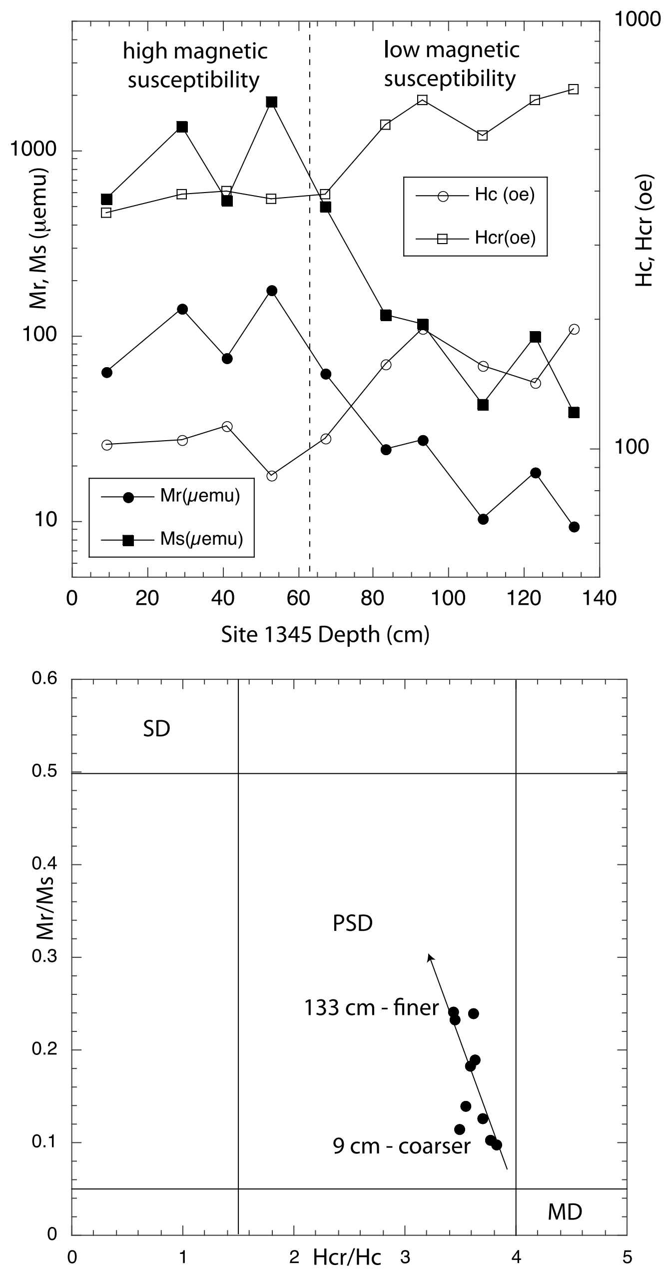

Fig. 5. Magnetic hysteresis measurements on selected samples from Hole 1345 A. Top: magnetic hysteresis parameters versus depth. The dashed line marks the boundary between high magnetic intensity sediments at the surface and low magnetic intensity sediments below. Bottom: Ratios of magnetic hysteresis parameters define regions of overall magnetic grain size. Regions of single-domain (SD) magnetic grains (finest grains, muds), pseudo-single domain (PSD) magnetic grains (muds-silts) and multi-domain (MD) magnetic grains (silts-sands) are shown.

higher concentrations of magnetic material, and lower (higher) Hc and Hcr, indicative of coarser (finer) grained magnetic material. Both of these relationships are consistent with the rock magnetic data in Fig. 4.

Ratios of these parameters were used to estimate domain state and hence magnetic grain size of the magnetic particles (Day et al., 1977; Dunlop, 2002a, b). Fig. 5 (bottom) plots Mrs/Ms versus Hcr/Hc for all samples. Other studies (e.g. Day et al., 1977; Dunlop 2002a, b) have documented the dominant magnetic grain size in individual parts of this plot. The smallest magnetic grains, single domain (SD) plot in the upper left and the coarsest magnetic grains, multidomain (MD), plot in the lower right. Our samples plot in between these two regions and are usual referred to as pseudosingle domain (PSD). Our samples start (9 cm) as high magnetic intensity with coarser grains closer to the MD region, and end (133 cm) with values that are finer and closer to SD/PSD. These hysteresis parameters also are consistent with our u-channel rock magnetic measurements of magnetic grain size discussed above.

5. Clastic grain size analysis

We have also carried out more traditional clastic grain size analysis to further test our rock magnetic grain size analysis. We have used selected samples from U1345 for this assessment. Grain size was measured using a Malvern Mastersizer 2000 grain size analyzer coupled to a Hydro 2000G. Each sample was pretreated with ≥30 mL of 30% H2O2 to remove organic matter, 10 mL of 1 M HCl to remove carbonate, and 10 mL of 1 M NaOH to remove biogenic silica. A tuff standard (TS2: n = 9525, $\bar{x}$ = 4.61 ± 0.18) was run twice at the beginning of each day, once every ten samples, and once at the end of every day to evaluate the equipment's analytical stability over time. All data are reported as percent by volume and divided into 10 grain-size intervals as well as d (0.1), d (0.5), d (0.9), and mode."

Fig. 6 (top) shows the weight % clay, silt, and sand and mode of each sample as a function of depth in U1345. The vertical line in Fig. 6 (top) is the boundary between high intensity sediments at the surface and low intensity sediments below. There is a very obvious one-for-one correspondence between high magnetic intensity (and coarser magnetic grain size) sediments and coarser clastic sediment versus low magnetic intensity (and finer magnetic grain size) sediments and finer clastic sediments. This difference is highlighted by plotting the actual clastic grain size distribution for all samples in Fig. 6 (bottom) where solid dots represents samples from the high magnetic intensity surface sediments and open dots represent samples from the low intensity deeper sediments. The mean grain size of the coarser clastic sediments is 50–60 μm (sand) while the mean grain size of the finer clastic sediments is 15–20 μm (silt).

6. Magnetic mineralogy

To further address the issue of magnetic mineralogy, we have recovered magnetic separates from five horizons in Hole U1345A: 0.07, 0.27, 1.55, 4.55, and 8.30 m CCSF. All magnetic separates were heated to 700 °C in a KLY-4 kappabridge and resulting thermomagnetic curves are shown in Fig. 7. These measurements indicate that the dominant magnetic mineral in all samples is magnetite. There is minor evidence for another magnetic mineral with Curie temperatures in the 250°C–350 °C range. This component is less than 10% of magnetite in intensity and could be either a second siliciclastic mineral or an authigenic mineral, which could be an iron sulfide (Roberts, 1995). Paleomagnetic studies (Lund et al., 2016) show that the NRM has a single characteristic remanence direction, which demagnetizes to the origin after ~20 mT af demagnetization at all sites. We interpret the characteristic remanence to be associated with magnetite. There is also a ubiquitous viscous overprint present, which is demagnetized by ~20 mT. The most likely source of this VRM is the coarser magnetic material (>10–15 μm), almost all magnetite, that is ubiquitously present in both the finer/lower-intensity and coarser/higher-intensity sediments.

7. Early sediment diagenesis

Porewater geochemistry measurements made during shipboard operations (Takahashi et al., 2011; Wehrmann et al., 2011) have documented a distinctive pattern of early sediment diagenesis (Roberts, 2015) that is seen at all the Bering Slope sites. This pattern is illustrated at Hole U1345B in Fig. 8. The bottom waters at all sites are oxygenated, although sometimes at low levels. The sediments, however, appear to be anaerobic almost to the sediment/water interface. This is indicated by porewater ferrous iron (Fe^{2+}) and manganese (Mn^{2+}) in the porewater.

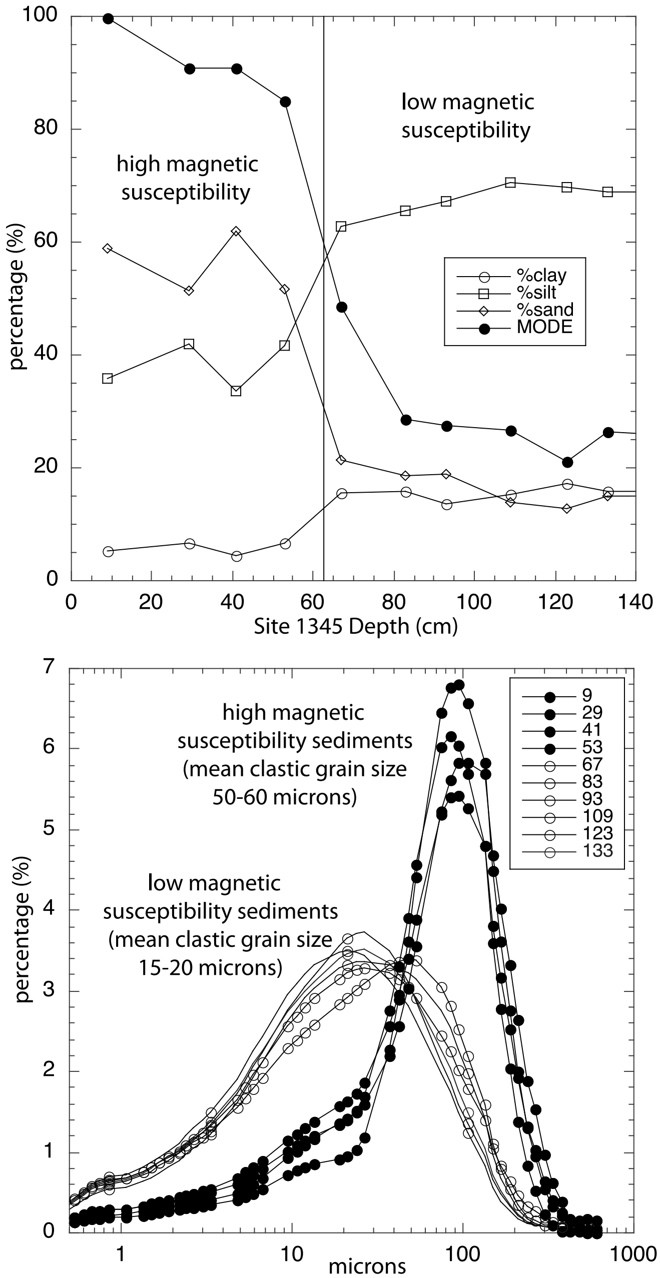

Fig. 6. Clastic grain size analysis of selected samples from Hole 1345 A. top: statistical measures of each grain size distribution plotted versus depth. The solid vertical line marks the boundary between high magnetic intensity sediments at the surface and low magnetic intensity sediments below. Bottom: Complete grain size distributions for all samples; open circles are low magnetic intensity samples; closed circles are high magnetic intensity samples.

Sulfate reduction starts within 1 m of the sediment/water interface and continues to a depth of ~6 m. Below that, sulfate concentrations are zero and methane (CH_4) begins to appear in the porewater. This boundary is termed the sulfate/methane transition zone (SMTZ) and separates zone of sulfate reduction above from the zone of methanogenesis below.

These chemical conditions must have some affect on the iron bearing magnetic minerals we study (Roberts, 2015). The anoxic porewater should present conditions that support dissolution of the finest-grain magnetic minerals (e.g., Canfield and Berner, 1987; Karlin and Levi, 1985; Leslie et al., 1990). Ferric phases should be dissolved first followed by ferrous phases, primarily magnetite. The ferrous iron freed in this process will most likely join with sulfide gas formed during sulfate reduction to form solid-phase iron sulfide minerals (e.g., Roberts, 1995). Some of these minerals are magnetic (e.g., greigite) while others are not (e.g., mackinowite). We have not identified any significant magnetic mineral component besides magnetite. Our paleomagnetic studies (Lund et al., 2016) support the notion that magnetic remanence is in magnetite and that it is a detrital signal that preserves magnetic field directional variability. Besides, only mud size (<5 μm) magnetite grains are readily susceptible to dissolution (Canfield and Berner, 1987; Karlin and Levi, 1985; Leslie et al., 1990; Roberts, 2015). Our clastic grain size analysis indicates that <5 μm clastic grains account for less than 5% of our clastic distributions in both coarse (sand size on average) and finer grained (silt size on average) sediments.

8. Discussion

Coarse-grained siliciclastic sediments come primarily from shelf sediment derived from the neighboring continental margins (e.g., Sharma, 1975; Seibold and Berger, 1996). The flux of this shelf sediment to the deep sea must be controlled by shelf processes and climate – short-term storminess, sea-ice formation on the Bering Sea shelf, and sea level (e.g., Carlson and Karl, 1985; Seibold and Berger, 1996). High seasonal to full-time sea ice on the shelf will limit shelf and direct river-derived continental sediments from reaching the deep basin. Similarly, low sea levels, extended permafrost conditions, and extensive permanent sea ice during the glacials (e.g., Caissie et al., 2010) will prevent most continental and shelf siliciclastic sediment from reaching the basin. On this basis, we associate high-intensity rock magnetic intervals with the ability for shelf sedimentation to at least intermittently reach the deep basin sites during interglacial to interstadial environmental conditions.

The low intensity sediments are commonly associated with finer-grained and much more well-sorted siliciclastic sediments (silts), which may also have significant (~10%–30%) biogenic components (Takahashi et al., 2011). We presume that the siliciclastic sediments are more strongly controlled by slope deposition or intermediate to deep-water flow with drift-deposit type deposition of more well-sorted and fine-grained siliciclastic material (e.g., Carlson and Karl, 1985; Seibold and Berger, 1996; Sommerfield et al., 2007). The finer grain size distribution is consistent in range and mean grain size to North Atlantic deep-sea sediment deposited as drift deposits by contourite deposition (Heezen and Ruddiman, 1966; Johnson et al., 1988). The general lack of coarser siliciclastic silts suggests that shelf siliciclastic flux is minimal in these sediments and that they are more likely associated with glacial or stadial environmental conditions.

These observations are consistent with the glacial/interglacial variations in clastic flux to the Meiji Drift, which are sediments derived from deep-ocean circulation and sediment scouring in the Bering sea (VanLaningham et al., 2009). The Meiji Drift sediments appear to be bimodal with a significant fraction of young volcanic arc rocks being advected during interglacials and older source rocks dominating during the glacials. The interglacial flux of younger volcanic arc rocks can be associated with clastic flux from the Bering Sea shelves and the older source rocks, perhaps, with scouring of the Bering Sea sediments from intermediate to deep water depth. The much better clastic grain size distribution and sorting during glacials (Fig. 6 bottom) is consistent with the sorting of North Atlantic drift deposits in both overall clastic grain size and mean grain size (Heezen and Ruddiman, 1966; Johnson et al., 1988).

Another element in the Bering Sea pattern of clastic sedimentation is the more complex timing of ‘glacial/stadial’ finer versus ‘interglacial/interstadial’ coarser sedimentation. Fig. 9 (bottom) shows the pattern of high/low magnetic intensity (chi) for the last 400 ka from site 1345 (Lund et al., 2016). It is clear that the high/low intensity oscillation is more complicated than simple glacial/interglacial variability. There are high/low intensity cycles within both glacial and interglacial intervals. High intensities are more prevalent in interglacials and low intensities

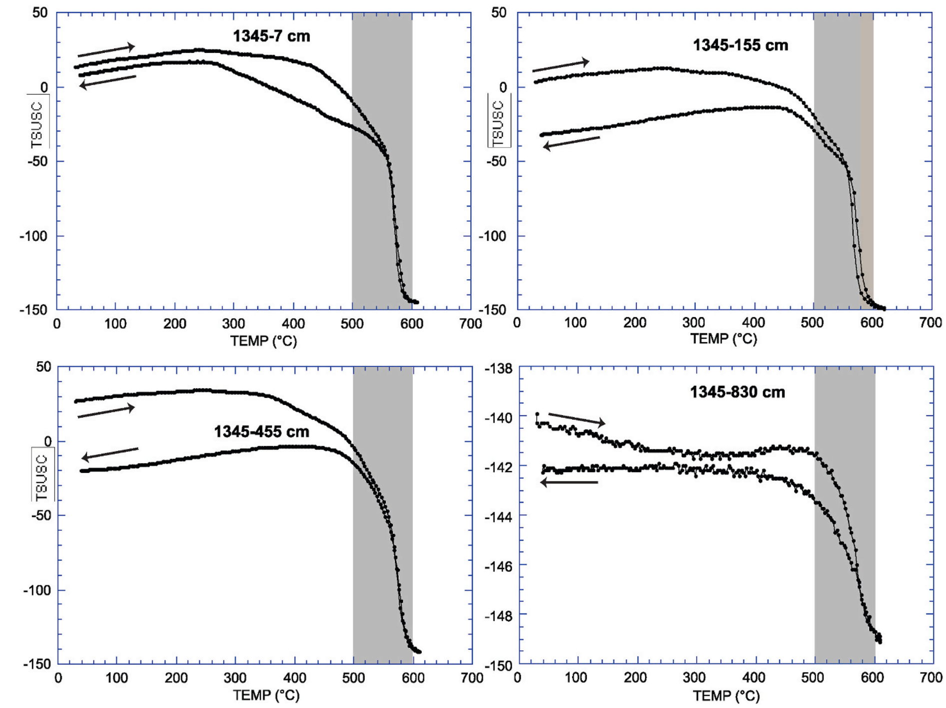

Fig. 7. Thermomagnetic curves for four magnetic separates from Hole U1345A.

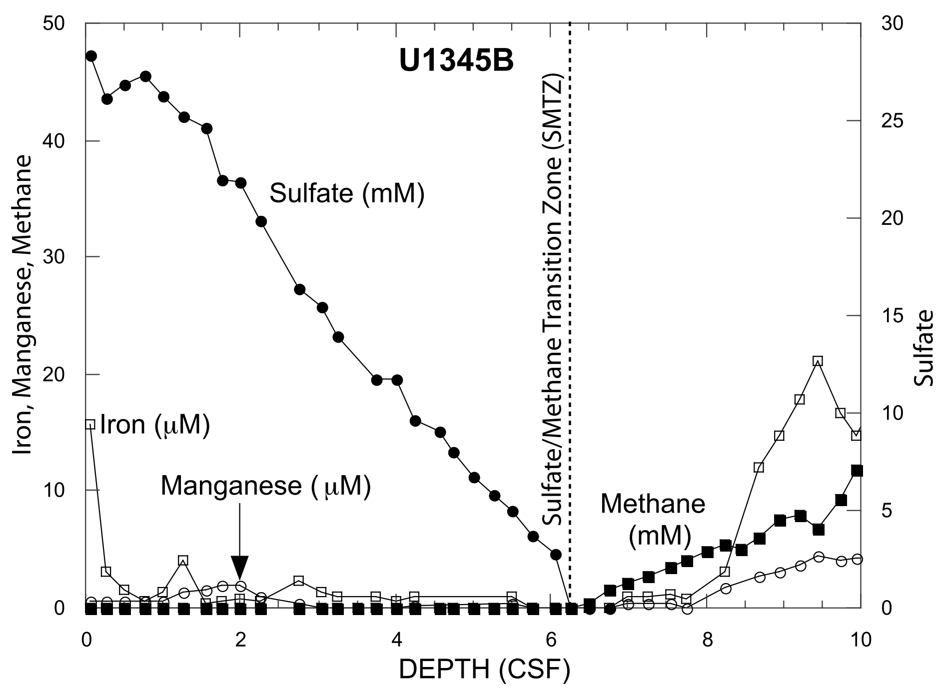

Fig. 8. Porewater geochemistry of Hole U1345B. The bottom waters at all sites are oxygenated, although sometimes at low levels. The sediments, however, appear to be anaerobic almost to the sediment/water interface. This is indicated by porewater ferrous iron (Fe^{2+}) and manganese (Mn^{2+}) in the porewater. This pattern is similar to that seen at all the Bering Slope Sites.

are more prevalent in glacials.

Lake Elgygytgyn in Siberia (Brigham-Grette et al., 2013; Frank et al. (2013); Melles et al., 2012; Nowaczyk et al., 2002, 2007, 2013), about 1000 km to the NW from the Bering Sea, shows a remarkably similar pattern of clastic sedimentation to the lake both in timing and bimodal pattern. Fig. 9 (top) shows magnetic intensity (chi) versus time for Lake Elgygytgyn. Nowaczyk et al. (2002, 2007) have interpreted the bio-modal oscillation in magnetic intensity to be primarily due to variable anoxia and ice cover in the lake. Warmer periods with, at least, intermittent open lake conditions permit clastic flux to the lake and higher magnetic susceptibility values. Colder periods with almost permanent ice cover to the lake had higher biological productivity that caused magnetic mineral dissolution and low magnetic susceptibility.. Nowaczyk et al. (2002, 2007) consider Milankovich (precessional) variations in insolation to be the primary cause of variable ice concentrations and open/closed lake conditions. We think such a scenario make sense for

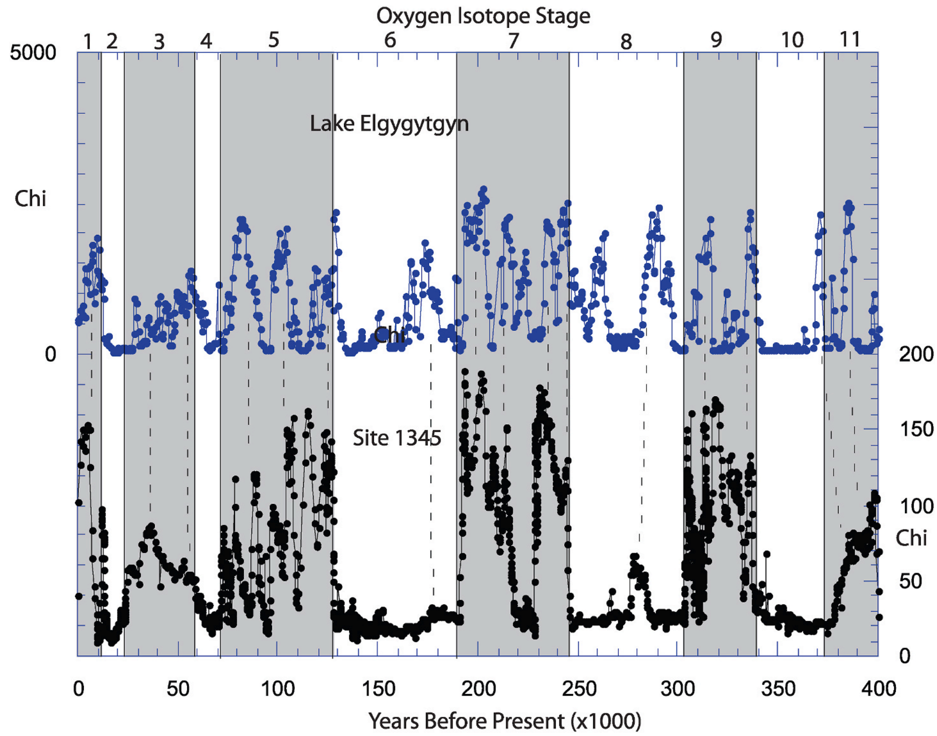

Fig. 9. Magneti intensity of Site 1345 and Lake Elgygytgyn for the last 400 ka. Both sites share a similar pattern of bimodal high/low magnetic intensity, noted by dashed lines. High magnetic intensities are more common in interglacial/interstadial intervals while low magnetic intensities are more common in glacial/stadial intervals.

the timing/extent of sea ice in the Bering Sea, as well. Although, we do see evidence in the clastic rich intervals for finer-scale sub-Milankovich variability as well. However, the chronology of Ex. 323 sediments is not yet good enough to be certain about either exact timing of rock magnetic variability or durations of individual high-magnetic intensity intervals.

9. Summary

IODP Expedition 323 recovered deep-sea sediments from seven sites in the Bering Sea. Initial shipboard measurements noted a dramatic bimodal distribution in rock magnetic intensity (both NRM and Chi) at all sites (Takahashi et al., 2011). High intensities were associated with glacial intervals and low intensities were associated with interglacial intervals. The distinctive rock magnetic intensity variability was correlated among all sites and used to help date and correlate the seven sites (Takahashi et al., 2011; Lund et al., 2016). Later oxygen isotope studies indicate that chronology was mistaken (Asahi et al., 2016; Cook et al., 2016).

We have now completed more detailed paleomagnetic and rock magnetic measurements on selected u-channeled sediments from these sites. Our new analysis indicates that the shipboard correlations were largely correct. But now, the intervals of high magnetic intensity are generally associated with Interglacial/Interstadial environmental conditions, while the intervals of low magnetic intensity are generally associated with Glacial/Stadial conditions.

U-channel rock magnetic measurements indicate that the high-intensity sediments contain relatively coarser magnetic grains (sand/silt) associated with coarser siliciclastic sediments while the low-intensity sediments contain finer magnetic grains (silt) associated with finer siliciclastic sediments. We associate the coarser magnetic grains and overall coarser clastic sediments with warmer intervals when more open water conditions permit sediment flux from the continental shelves. The finer magnetic grains and associated finer clastic sediment is largely derived from sediment reworking and redeposition associated with slope processes and deep-sea contour currents when ice cover is more permanent. We have corroborated the grain size variability with magnetic hysteresis measurements and clastic grain size analysis. The clastic grain size distributions of the coarser versus finer grained sediments are significantly different; coarser grained sediments have a broad grain size distribution with 50–60 μm mean grain size, while finer grained sediments have a much more narrow grain size distribution with 15–20 μm mean grain size. The finer grain size distribution is consistent in range and mean grain size to North atlantic sediment deposited as drift deposits by contourite deposition (Heezen and Ruddiman, 1966; Johnson et al., 1988).

The dominant magnetic mineral in all sediments is detrital magnetite. Early sediment diagenesis plays a minor role in the overall rock magnetic variability of the Bering Sea deep-sea sediments. This is largely due to the coarse grain size of the sediments (silts/sands). Early diagenesis tends to act most strongly on the finest grained magnetic material (less than a few microns), which constitutes less than a few percent of our studied sediments.

The magnetic variability that we see in the Quaternary Bering Sea sediments appears to be comparable to other studies from this region. VanLaningham et al. (2009) attribute deposition of the Meiji drift, directly south of the deep water exit from the Bering Sea, to sediments derived from the Bering Sea. They see a bimodal distribution in the types of sediments that are deposited with younger arc rocks during interglacials and older continental rocks during glacials. That is consistent with our coarser Interglacial) magnetic sediments derived primarily from shelf rocks rich in recent volcanics versus deeper Bering Sea sediments associated with reworking of older Bering Sea sediments during the glacials. We also note the strong similarity in timing of strong versus weak magnetic intensity sediments of Lake Elgygytgyn, about 1000 km to the NW of the Bering Sea, Both seem to be controlled by the degree of intermittent open water conditions, more so in the interglacials and very little in the glacials.

Declaration of competing interest

The authors declare the following financial interests/personal relationships which may be considered as potential competing interests:

This is a manuscript that summarizes research done by a group of individuals with NSF funding

Acknowledgements

This work was supported by grants JOIDES-USSSP: 03/01/2010-03/01/2012 and NSF-OCE0962385: 06/15/2010.

References

Brigham-Grette, J., Melles, M., Minyuk, P., Andreev, A., Tarasov, P., DeConto, R., Koenig, S., Nowaczyk, N., Wennrich, V., Rosén, P., Haltia, E., Cook, T., Gebhardt, C., Meyer-Jacob, C., Snyder, J., Herzschuh, U., 2013. Pliocene warmth, polar amplification, and stepped pleistocene cooling recorded in NE arctic Russia. Science 340 (6931), 1421–1427. https://doi.org/10.1126/science.1233137.

Caissie, B., Brigham-Gette, J., Lawrence, K., Herbert, t., Cook, M., 2010. Last glacial maximum to Holocene sea surface conditions at Unmak Plateau, Bering Sea, as inferred from diatom, alkenone, and stable isotope records. Paléo 25, PA1206.

Canfield, D.E., Berner, R.A., 1987. Dissolution and pyritization of magnetite in anoxic marine sediments. Geochem. Cosmochim. Acta 51, 645–659.

Carlson, P., Karl, H., 1985. Mass movement of fine-grained sediment to the basin floor, Bering Sea, Alaska. Geo Mar. Lett. 4, 221–225.

Cook, M., A.C. Ravelo, A. Mix, I. Nesbit, and N. Miller, this issue, Tracing Bering sea circulation with benthic foraminiferal stable isotopes during the pleistocene, Deep Sea Research II.

Day, R., Fuller, M., Schmidt, V.A., 1977. Hysteresis properties of titanomagnetites: grain-size and compositional dependence. Phys. Earth Planet. In. 13 (4), 260–267.

Dunlop, D.J., 2002a. Theory and application of the Day plot (Mrs/Ms versus Hcr/Hc) 1. Theoretical curves and tests using titanomagnetite data. J. Geophys. Res.: Solid Earth 107 (B3). EPM 4-1-EPM 4-22.

Dunlop, D.J., 2002b. Theory and application of the Day plot (Mrs/Ms versus Hcr/Hc) 2. Application to data for rocks, sediments, and soils. J. Geophys. Res.: Solid Earth 107 (B3). EPM 5-1-EPM 5-15.

Frank, U., Nowaczyk, N., Minyuk, P., Vogel, H., Rosén, P., Melles, M., 2013. A 350 ka record of climate change from Lake El'gygytgyn, Far East Russian Arctic: refining the pattern of climate modes by means of cluster analysis. Climate 9 (4), 1559–1569. https://doi.org/10.5194/cp-9-1559-2013.

Heezen, B.C., Hollister, C.D., Ruddiman, W.F., 1966. Shaping the continental rise by deep geostrophic contour currents. Science 152, 502–508.

Johnson, T.C., Lynch, E.L., Showers, W.J., Palczuk, N.C., 1988. Pleistocene fluctuations in the western boundary undercurrent on the blake outer ridge. Paleoceanography 3, 191–207.

Joseph, L., Rea, D., van der Pluijm, P., 1998. Use of grain size and magnetic fabric analyses to distinguish among depositional environments. Paléo 13, 491–501.

Karlin, R., Levi, S., 1985. Geochemical and sedimentological constriants on the magnetic properties of hemipelagic sediments. J. Geophys. Res. 90, 10373–10392.

Keigwin, L., Jones, G.A., 1989. Glacial-Holocene stratigraphy, chronology, and paleoceanographic observations on some North Atlantic sediment drifts. Deep Sea Res., Part A 36, 845–867.

Leslie, B., Lund, S., Hammond, D., 1990. Rock magnetic evidence for the dissolution and magnetic growth of magnetic minerals within anoxic sediments of the California continental borderland. J. Geophys. Res. 95, 4437–4452.

Lund, S., Gorsline, D.L., Henyey, T.L., 1992. Rock magnetic characteristics of surficial marine sediments from the California continental borderland. Earth Planet Sci. Lett. 108, 93–107.

Lund, S., Stoner, J., Mix, A., Tiedemann, R., Blum, P., the Leg 202 Shipboard Party, 2003. Observations on the effect of a nonmagnetic core barrel on shipboard paleomagnetic data: results from ODP leg 202. In: Initial Results from ODP Leg 202, vol. 202. Ocean Drilling Program, College Station, TX.

Lund, S., J. Stoner, M. Okada, and E. Mortazavi, This Issue, Paleomagnetic field variability and chronostratigraphy of Brunhes-Epoch deep-sea sediments from the Bering Sea: IODP Expedition 323, Deep Sea Research II.

Melles, M., Brigham Grette, J., Minyuk, P.S., Nowaczyk, N., Wennrich, V., DeConto, R. M., Anderson, P.M., Andreev, A.A., Coletti, A., Cook, T.L., Haltia Hovi, E., Kukkonen, M., Lozhkin, A.V., Rosén, P., Tarasov, P., Vogel, H., Wagner, B., 2012. 2.8 million years of arctic climate change from Lake El'gygytgyn, NE Russia. Science 337 (6092), 315–320.

Nagashima, K., Asahara, Y., Takeuchi, F., Harada, N., Toyoda, S., 2012. Contribution of detrital materials from the Yukon River to the continental shelf sediments of the Bering Sea based on electron spin resonance. Deep Sea Res. Part II 61–64, 145–154.

Nowaczyk, N., Haltia, E.M., Ulbricht, D., Wennrich, V., Sauerbrey, M.A., Rosén, P., Vogel, H., Francke, A., Meyer-Jacob, C., Andreev, A.A., Lozhkin, A.V., 2013. Chronology of Lake El'gygytgyn sediments – a combined magnetostratigraphic, palaeoclimatic and orbital tuning study based on multi-parameter analyses. Clim. Past 9, 2413–2432. https://doi.org/10.5194/cp-9-2413-2013. DOI: http://doi.org/10.1126/science.1222135.

Nowaczyk, N., Melles, M., Minyuk, P., 2007. A revised age model for core PG1351 from Lake El'gygytgyn, Chukotka, based on magnetic susceptibility variations tuned to northern hemisphere insolation variations. J. Paleolimnol. 37 (1), 65–76. https://doi.org/10.1007/s10933-006-9023-8.

Nowaczyk, N., Minyuk, P., Melles, M., Brigham-Grette, J., Glushkova, O., Nolan, M., Lozhkin, A.V., Stetsenko, T.V., Andersen, P.M., Forman, S.L., 2002. Magnetostratigraphic results from impact crater Lake El'gygytgyn, northeastern Siberia: a 300 kyr long high-resolution terrestrial palaeoclimatic record from the Arctic. Geophys. J. Int. 150 (1), 109–126. https://doi.org/10.1046/j.1365-246X.2002.01625.x.

Roberts, A., 1995. Magnetic properties of sedimentary greigite. Earth Planet Sci. Lett. 134, 227–236.

Roberts, A., 2015. Magnetic mineral diagenesis. Earth Sci. Rev. 151, 1–47.

Sharma, G., 1975. Contemporary epicontinental sedimentation and shelf grading in the Southeast Bering Sea. GSA (Geol. Soc. Am.) Spec. Pap. (Reg. Stud.) 151, 33–48.

Seibold, E., Berger, W., 1996. The Sea Floor – an Introduction to Marine Geology. Springer, p. 356.

Sommerfield, C., Ogston, A., Mullenbach, B., Drakes, D., Leithold, E., 2007. Oceanic dispersal and accumulation of river sediment. In: Continental Margin Sedimentation, vol. 37. SEPM Special Pub, pp. 157–205.

Takahashi, K., 2005. The Bering sea and paleoceanography. Deep Sea Research II 52, 2080–2091.

Takahashi, K., Ravelo, A., Alvarez, C., 2011. Zarikian, and the expedition 323 scientists. In: Proceedings of the Integrated Ocean Drilling Program: Expedition Reports: Bering Sea Paleoceanography, p. 323. https://doi.org/10.2204/iodp.proc.323.2011.

Tanaka, S., Takahashi, K., 2005. Late Quaternary paleoceanographic changes in the Bering Sea and the western subarctic Pacific based on radiolarian assemblages. Deep Sea Research II 52, 2131–2149.

VanLaningham, S., Pisias, N., Duncan, R., Clift, P., 2009. Glacial-interglacial sediment transport to the Meiji drift, northwest pacific ocean: evidence for timing of beringian outwashing. Earth Planet Sci. Lett. 277, 64–72.

Wagner, C., Bennett, K., de Vernal, A., Forwick, M., Fritz, M. Heikkla, et al., 2015. Variability in transport of terrigenous material from the shelves and the deep Arctic Ocean during the Holocene. Polar Res. 34, 24964.

Wehrmann, L., Risgaard-Peterson, N., Schrum, H., Walsh, E., Huh, Y., Ikehara, M., Pierre, C., D'Hondt, S., Ferdelman, T., Ravelo, A., Takahashi, K., Alvarez Zarikian, C., the IODP Expedition 323 Scientific Party, 2011. Coupled organic and inorganic carbon cycling in the deep subseafloor sediment of the Northeastern Bering Sea Slope (IODP Expedition 323). Chem. Geol. 284, 251–261.